Multi-Objective Optimization of Solid Oxide Fuel Cell/Gas Turbine Combined Heat and Power System: A comparison between Particle Swarm and Genetic Algorithms

Sadegh Safari [1], Taher Hajilounezhad [2,*], Mehdi Ali Ehyaei [3]

[1] School of the Environment and Energy, Islamic Azad University- Science and Research Branch, Tehran, Iran.

[2] Department of Mechanical & Aerospace Engineering, University of Missouri, Columbia, MO, USA

[3] Department of Mechanical Engineering, Pardis Branch, Islamic Azad University, Pardis New City, Iran

ABSTRACT

Many studies have attempted to optimize integrated Solid Oxide Fuel Cell-Gas Turbine (SOFC-GT), although different and somehow conflicting results are reported employing various algorithms. In this study, Multi-Objective Optimization (MOO) is employed to approach the optimal design of SOFC-GT considering all prevailing factors. The emphasis is placed on the evaluation of the Particle Swarm Optimization (PSO) and Genetic Algorithm (GA) performance as two effective approaches for solving the multi-objective and non-linear optimization problems. Multi- objective optimization is carried out on two vital objectives; the electrical efficiency and the overall output power of the system. The considerable achievements are the set of optimal points that aim to identify the system optimal performance which provides a practical basis for the decision-makers to choose the appropriate target functions. For the studied conditions, the two algorithms nearly exhibit similar performance, while the PSO is faster and more efficient in terms of computational effort. The PSO appears to achieve its ultimate parameter values in fewer generations compared to the GA algorithm under the examined circumstances. It is found that the maximum power of 410 kW is accomplished employing the GA optimization method with an efficiency of 64%, while PSO method yields the maximum power of 419.19 kW at the efficiency of 58.9%. The results stress that PSO offers more satisfactory convergence and fidelity of the solution for the SOFC-GT MOO problems.

Keywords: Modeling; Solid oxide fuel cell; Gas turbine; Multi-Objective Optimization; Heat recovery steam generation

1. INTRODUCTION

Renewable energy generation methods have been intensively studied in recent years. However, solid oxide fuel cells (SOFC) have been extensively interrogated and developed since they work at high temperatures. This provides the opportunity of hybrid concepts employment such as the integrated gas turbine (GT) and SOFC leading to a considerable improvement of the overall system

[*] Corresponding author:
E-mail address: thnrf@mail.missouri.edu (T. Hajilounezhad)
ORCID: 0000-0002-8688-8148 (T. Hajilounezhad)

efficiency [1]. Combining internal combustion engines or SOFC with GT, the gaseous fuel can be converted to heat and power. However, the combination of SOFC and GT yields better performance [2-5]. This hybrid energy conversion system will provide superior utilization of natural resources that considerably decreases harmful impacts on the environment as well as making higher profit [6-8].

Typically, the optimization of the integrated SOFC/GT deals with various objectives which sometimes may be conflicting like capital investment, operating cost, output power, efficiency, energy consumption, and environmental considerations. In such circumstances, multi-objective optimization (MOO) turns out a promising approach for finding various Pareto optimal solutions, to comprehend the quantitative tradeoffs between the objectives and also to acquire the optimal values of decision variables [6, 9, 10]. However, various arrangements of SOFC-GT combined systems have been studied with respect to several design parameters [11-15]. The SOFC-GT hybrid systems are usually fueled by natural gas, converted by means of an internal reformer. This will dramatically reduce the system capital expense due to eliminating any external fuel processing [16].

Nevertheless, some researchers have interrogated the thermodynamic modeling of SOFC/GT combined system [16-20], while others focused on the optimization of these systems, suggesting various design configurations. A synthesis/design optimization of an integrated GT-SOFC power plant has been performed by Calinse et al. [14], where a classical single-level method created on the GA basis has been developed. A thermo-economic optimization that employs a Lagrange Multiplier Approach (LMA) has been examined by Cheddie [15]. In this work, an indirectly coupled integrated SOFC-GT power plant was considered where sizing and operating conditions were employed as the decision variables to obtain the minimum lifecycle cost of the system.

Autissier et al. [21] have performed the optimization for the design of hybrid SOFC-micro GT considering two objectives; boosting the energy efficiency and deceasing the cost. The optimization results exhibit designs with costs ranging from 2400 $/kW for a 44% energy efficiency to 6700 $/kW for a 70% energy efficiency. Sabramanyan et al. [22] have performed multi-objective optimization for a conceptual layout of a SOFC-proton exchange membrane fuel cell (PEMFC) hybrid power plant. Optimizing the design of SOFC system involves consideration of the cost and performance of a SOFC-PEMFC based on a novel algorithm for minimization of single objective optimization problems (MINSOOP).

Table 1 lists a review of the literature regarding the optimization methods and strategies for SOFC/GT hybrid systems. It offers the decision variables, parameters that have been taken into consideration, objectives, the optimization method and the outstanding results for hybrid applications [23].

Although different optimization methods have been applied to SOFC/GT systems, none has compared the performance of these optimization methods. This work presents two optimization algorithms based on the intelligent approaches for an integrated SOFC-GT system to optimize the efficiency of the system, i.e. simultaneously maximizing the power output and the overall efficiency.

At first, the integrated system was modeled in MATLAB to assess the performance characteristics of the system and thereby the system components have been evaluated to examine the efficiency of the system. Since the efficiency of the SOFC-GT hybrid system is defined as the ratio of the generated power of the system to the fuel input, it is a function of several variables. Two different optimization algorithms were employed to accomplish the optimal operating conditions of the entire system. As the system is extremely nonlinear, due to the combination of two extremely nonlinear systems, artificial intelligence should be employed to optimize the overall system performance.

GA and PSO were used as two most common and effective approaches among various existing intelligent algorithms. Both algorithms are population-based heuristic search methods that proceed towards the optimal solution by updating generations. Also, they are assumed to obtain a solution to the given objective functions by employing different methodologies while interactively comparing their implementation and the results. The concurrent implementation of GA and PSO for the optimization of the combined SOFC-GT system provides an optimization framework that can be easily extended to the optimization of other complicated energy systems [24].

As discussed earlier, there are a variety of studies that have aimed to optimize SOFC/GT cost versus power or cost versus efficiency, while only a few of them examine these two objective functions by a MOO approach for the optimization purposes. Since not all prevailing factors have been comprehensibly studied, it is still necessary to apply MOO on the SOFC/GT system. Although some researches examined the output power and cost or the system efficiency and cost as the objective functions, there is no reported study to focus on the optimization of efficiency and output power, as two more impactful and conflicting objectives while considering fuel utilization, pressure ratio, steam to carbon ratio, and fuel flow rate as the decision variables. Also, to the best of our knowledge, PSO and GA have been rarely compared directly in the previous studies, although they are applied individually for the other renewable energy systems like SOFC/GT CHP system.

To establish the optimization framework, first the thermodynamic model of SOFC-GT hybrid system is described. Then, the multi-objective optimization is discussed and implemented to the proposed system. The MOO is applied based on the simultaneous determination of the optimal performance and operation conditions through employing two different optimization methods, i.e. the GA and the PSO. The considerable accomplishments of the recommended MOO approaches are set of optimal points (Pareto frontier) that target to determine the SOFC/GT optimal performance and operation conditions. Undoubtedly, Pareto frontiers offer critical information for the decision-making process, as the most remarkable and beneficial achievement of this work.

Briefly, the main purposes of this research can be explained as:

- Developing an efficient energy system based on SOFC/GT for CHP applications
- Interrogating the effects of steam to carbon ratio, compressor pressure ratio, fuel utilization factor on the electrical efficiency and the output power
- Applying MOO to examine the optimal operation conditions of the designed system using both PSO and GA for determining the best solutions
- Systematically exploring and comparing the Pareto frontiers with regard to two heuristics algorithms to investigate the optimal range of the influential parameters
- Providing a practical basis for decision-makers to choose among the target functions in accordance with the optimal performance requirements

Eventually, the results of optimization methods are presented and compared. The results include the changes in power output and efficiency of the hybrid system over the iterations employing GA and PSO. Also, the Pareto diagram for both GA and PSO approach is presented. In summary, the innovations of this paper are:

- Implementation of two new objective functions (efficiency and output power) to maximize the power generation and energy efficiency of the system

- Optimization of the system including SOFC, gas and steam cycle by two optimization algorithms, i.e. PSO and GA
- Comparison of the optimization results from the employed algorithms to select the best approach as the most effective tool in this type of cycles
- Sensitive analysis of the optimization results

2. MATERIAL AND METHODS

2.1 System description

The schematic block diagram of the suggested SOFC-GT hybrid system is depicted in Fig. 1. The system layout is divided into two main subsystems: SOFC and GT. The system includes other auxiliary equipment such as a heat recovery steam generator (HRSG), fuel compressor, inverter, and heat exchangers. Compressed fuel is reformed into a rich hydrogen gas in an internal reforming unit, then the gas is transported into the anode compartment of the SOFC stack. In the SOFC, reformed fuel will be converted to electricity directly and DC power will be generated by an electrochemical reaction occurring within the stack, and subsequently, the generated power will be turned to AC power by employing an inverter. A portion of this electricity is utilized to provide the power source for the fuel compressor. The compressed air is used as SOFC cathode gas, after being preheated in the heat exchanger.

Unreacted gases of the anode side and preheated compressed air of the cathode participate in the combustion reaction. Combustion products will be expanded in the gas turbine for both generating additional electrical power and producing mechanical work for running the compressor. Gas turbine exhaust flow will be recovered to preheat the compressed air as well as delivering the necessary heat in the HRSG to produce steam used by the internal reformer.

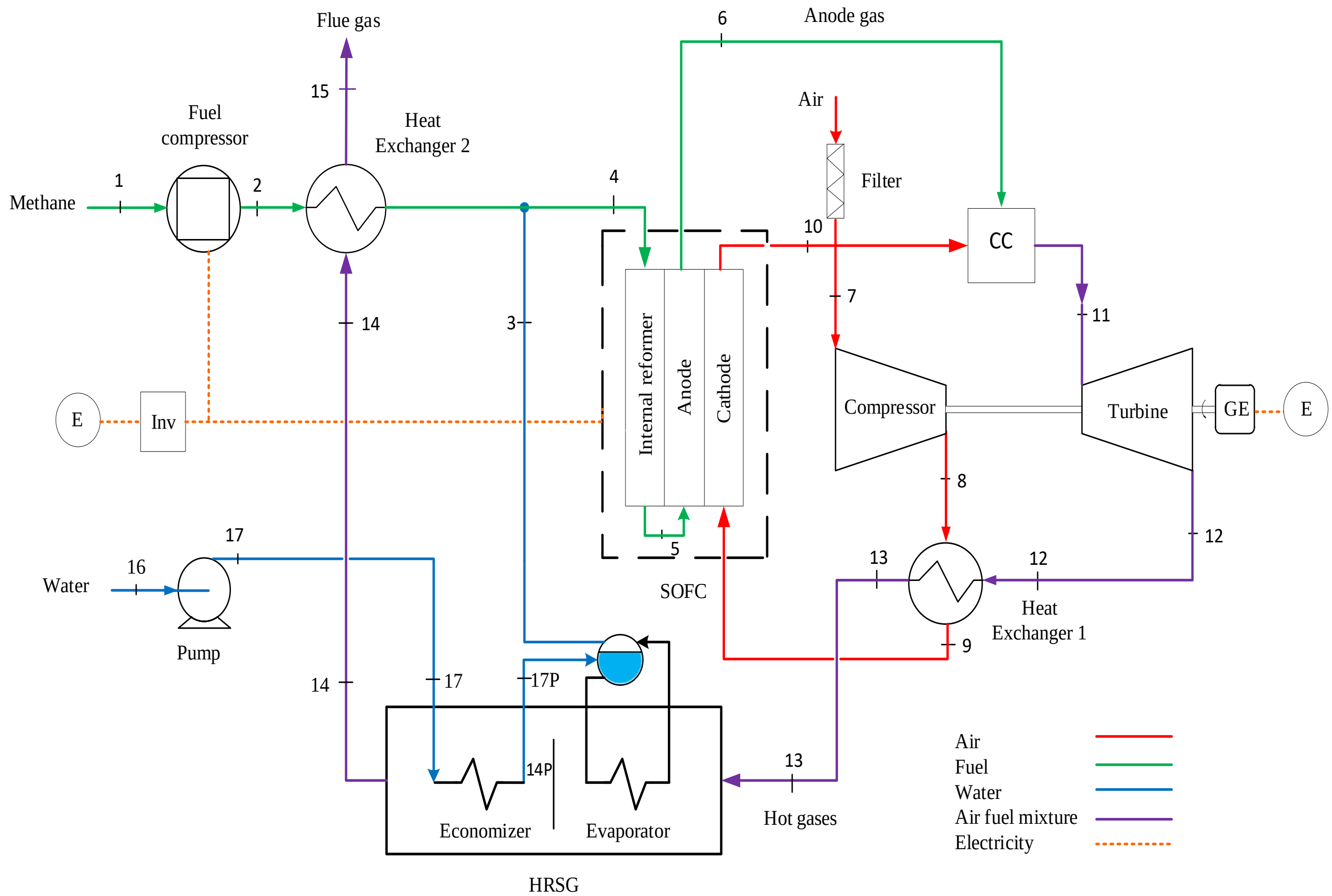

Fig. 1. The Schematic of SOFC-GT hybrid system.

2.2. Model assumptions

Principal assumptions for developing the proposed SOFC-GT hybrid system are listed as:

- Ideal gas assumption is considered for all gases.
- Steady state condition is considered for the operation of all system components.
- The working fluid in all parts of the cycle is assumed to work as an ideal gas
- Temperature, pressure, and gas compositions are uniformly distributed in each component.
- 5% pressure drop is assumed in the combustion chamber and the fuel cell stack.
- Pressure drop is presumed to be 4% and 5% for the heat exchangers and the HRSG, respectively.
- The inverter efficiency is assumed 0.98, the turbine mechanical efficiency is considered 0.8, the generator efficiency is presumed 0.97 and the efficiency of both air compressor and fuel compressor is assumed 0.78.

- Methane is selected as the supplied fuel to the system.
- The dead conditions are assumed P_0=101.3 kPa and T_0= 298 K

These assumptions are employed throughout the analysis to derive the corresponding equations of each system component [25, 26].

2.3. System modeling

The model is structured according to the zero-dimensional method in which the mass and energy balance equations are solved simultaneously.

2.3.1. Solid oxide fuel cell

In order to optimize the SOFC-GT integrated system parameters, it is vital to develop a SOFC model that is capable of predicting the performance based on its operating condition. The proposed SOFC is built on a tubular design which has been designed and demonstrated by Siemens-Westinghouse [27]. An electrochemical model that evaluates the power and efficiency of SOFC is developed. The geometric and material properties are selected from the literature [28].

The gas flow leaving the fuel compressor will enter the internal pre-reformer, then reforming and shifting reactions occur, i.e. ($CH_4 + H_2O \leftrightarrow 3H_2 + CO$) and ($CO + H_2O \leftrightarrow H_2 + CH_4$), respectively. The hydrogen produced from such reactions participates in the cell electrochemical reaction i.e. ($H_2 + \frac{1}{2} O_2 \rightarrow H_2O$); as a result, a portion of methane will be turned into hydrogen. These reactions are considered to proceed to chemical equilibrium.

The chemical and electrochemical reactions that take place at the anode and the cathode of the fuel cell may be obtained from the following equilibrium equations [29]:

$$x_r \rightarrow (CH_4 + H_2O \leftrightarrow 3H_2 + CO) \tag{1}$$

$$y_r \rightarrow (CO + H_2O \leftrightarrow H_2 + CH_4) \tag{2}$$

$$z_r \rightarrow (H_2 + \frac{1}{2} O_2 \rightarrow H_2O) \tag{3}$$

where x_r, y_r and z_r are the internal reformer conversion rates.

The fuel utilization factor, U_f, and the air utilization ratio, U_o, can be defined as follows [29]:

$$U_f = \frac{(\text{Fuel})_{\text{Consumed}}}{(\text{Fuel})_{\text{Supplied}}} = \frac{z_r}{3x_r + y_r} \tag{4}$$

$$U_o = \frac{(\text{Air})_{\text{Consumed}}}{(\text{Air})_{\text{Supplied}}} = \frac{z_r/2}{\dot{m}_{O_2.9}} \tag{5}$$

Employing the mass balance equations for each gas component, the molar flow rate will be achieved as follows [29]:

$$\dot{m}_{CH_4.5} = x_r \tag{6}$$

$$\dot{m}_{H_2O.5} = r_{sc} \cdot \dot{m}_{CH_4.5} \tag{7}$$

$$\dot{m}_{H_2.6} = 3x_r + y_r - z_r \tag{8}$$

$$\dot{m}_{CO.6} = x_r - y_r \tag{9}$$

$$\dot{m}_{CO_2.6} = y_r \tag{10}$$

$$\dot{m}_{H_2O.6} = \dot{m}_{H_2O.5} - x_r - y_r + z_r = (1 \cdot 5x_r - y_r + z_r) \tag{11}$$

$$\dot{m}_{O_2.9} = \frac{z_r}{2U_o} \tag{12}$$

$$\dot{m}_{O_2.10} = \dot{m}_{O_2.9} - \frac{z_r}{2} \tag{13}$$

$$\dot{m}_{N_2.9} = \frac{79}{21} \times \dot{m}_{O_2.9} \tag{14}$$

$$\dot{m}_{N_2.10} = \dot{m}_{N_2.9} \tag{15}$$

$$\dot{m}_9 = \dot{m}_{O_2.9} + \dot{m}_{N_2.9} \tag{16}$$

$$\dot{m}_{10} = \dot{m}_{O_2.10} + \dot{m}_{N_2.10} \tag{17}$$

$$\dot{m}_5 = \dot{m}_{H_2O.5} + \dot{m}_{CH_4.5} \tag{18}$$

$$\dot{m}_6 = \dot{m}_{H_2.6} + \dot{m}_{H_2O.6} + \dot{m}_{CO.6} + \dot{m}_{CO_2.6} \tag{19}$$

The constants x_r and y_r can be obtained employing equilibrium constant as well as the above equations, while shifting equilibrium constant can be written as [29]:

$$\ln K_s = -\frac{\Delta G^0}{\bar{R}T} = \ln\left[\frac{y_r \times (3x_r + y_r - z_r)}{(x_r - y_r) \times (1 \cdot 5x_r - y_r + z_r)}\right] \tag{20}$$

Maximum cell voltage is determined from equation (21). Therefore, Nernst voltage can be formulated as follows [25]:

$$V_{nernst} = -\frac{\Delta G^0}{2F} - \frac{\bar{R}T}{2F} \ln\left[\frac{p_{H_2O}}{p_{H_2}\sqrt{p_{o_2}}}\right] \tag{21}$$

where $\bar{R}$ is the universal gas constant, ΔG^0 indicates Gibbs free energy at standard conditions for the electrochemical reaction, F refers to Faraday's constant (96,485 $C\,mol^{-1}$), cell temperature is introduced by T and p indicates the partial pressure of respective species.

The operating voltage drops when the electric current is drawn from the cell, mainly due to some loss such as ohmic, activation and concentration polarization. They are individually categorized as electrochemical reaction activation, V_{act}; ohmic polarization, V_{ohm}; and concentration depletion, V_{Con}. Operating cell voltage, V_{Cell}, can be calculated as [25]:

$$V_{cell} = V_{nernst} - (V_{act} + V_{ohm} + V_{con}) \tag{22}$$

Activation polarization is calculated by the Butler-Volmer equation, expressed as [25]:

$$j = j_0 \left[\exp\left(\frac{\beta n_e F V_{act}}{RT}\right) - \exp\left(-(1-\beta)\left(\frac{n_e F V_{act}}{RT}\right)\right)\right] \tag{23}$$

where j indicates the current density, β is the transfer coefficient, and j_0 refers to exchange current density.

Ohmic polarization resulting from the electron and ion transmission processes is determined by the following equations based on Ohm's law [28]:

$$V_{Ohm} = i \sum_k r_k \tag{24}$$

$$r_k = \sum_k \frac{\rho_k \delta_k}{A} \tag{25}$$

$$\rho_k = \sum_k a_k \exp^{\left({b_k}/{T}\right)} \tag{26}$$

where r_k is the ohmic resistance, δ_k refers to the current flow length and ρ_k indicates the material resistivity. The coefficients of a and b are the characteristics of constituent materials

The concentration loss which is a result of the transport of gases to the electrodes will be calculated as follows [28]:

$$V_{con} = \frac{RT}{2F} \operatorname{Ln} \left(1 + \frac{p_{H_2}.j}{p_{H_2}.j_{lim}}\right) - \frac{RT}{2F} \operatorname{Ln} \left(1 - \frac{j}{j_l}\right) \tag{27}$$

where j_l is the limiting current density and j refers to the current density that will be estimated by the following electrochemical reaction [28]:

$$I = j \cdot A_c \tag{28}$$

$$j = \frac{n_e \cdot F \cdot z_r}{A_c} \tag{29}$$

where n_e is the number of electrons that are formed per hydrogen mole by electro-chemical reactions, A_c is the cell activation area, and I is the current. More details about calculation procedures of voltage, polarizations and current density may be found in [25, 28].

The electrical power generated from the SOFC may be calculated as [25]:

$$\dot{W}_{SOFC} = N \cdot I \cdot V_{Cell} \tag{30}$$

where N indicates number of cells. The net electrical power of the SOFC can be given as [25]:

$$\dot{W}_{SOFC,net} = \dot{W}_{SOFC} \cdot \eta_{inv} - \dot{W}_{FC} \tag{31}$$

Where, η_{inv} is the inverter efficiency which is assumed to be 0.98, and $\dot{W}_{FC}$ is the electrical power used by the fuel compressor.

Mass balance of SOFC considering input and output flows may be written as follows [30]:

$$\sum \dot{m}_i = \sum \dot{m}_e \tag{32}$$

$$\dot{m}_9 + \dot{m}_4 = \dot{m}_{10} + \dot{m}_6 = \dot{m}_9 + (\dot{m}_4 U_f) + \dot{m}_4(1 - U_f) \tag{33}$$

where $\dot{m}_4$ is the fuel mass flow rate injected to the SOFC and $\dot{m}_9$ is the air mass flow rate injected to SOFC. Alternatively, applying the first law of thermodynamic equation (33) can be rewritten as [30]:

$$\dot{m}_9 h_9 + (\dot{m}_4 U_f)LHV + \dot{m}_4(1 - U_f)h_4 - \dot{W}_{Fc} - \dot{m}_{10}h_{10} - \dot{m}_6 h_6 = 0 \tag{34}$$

where LHV stands for the lower heating value of methane that is about 50,000 ($^{kJ}/_{kg}$). It is noteworthy that all reactions are considered to be adiabatic.

The energy balance for the proposed hybrid system can be written as [30]:

$$\dot{m}_1 h_1 + \dot{m}_3 h_3 + \dot{m}_4 U_f LHV + \dot{Q}_{CC} - \dot{m}_{15}h_{15} - \dot{Q}_{Loss} - \dot{W}_{Fc} - \dot{W}_P - \dot{W}_{GT} = 0 \tag{35}$$

where $\dot{Q}_{CC}$ is the generated heat in combustion chamber, $\dot{Q}_{Loss}$ is the heat losses of the hybrid cycle, $\dot{W}_{Fc}$ and $\dot{W}_P$ are power used by the fuel compressor and pump, respectively, and $\dot{W}_{GT}$ is the output power generated by the gas turbine.

In order to solve the equations of the SOFC stack, first the cell current is calculated at a given current density. The quantity of hydrogen and oxygen necessary for the electrochemical reaction can be calculated at this identified current amount. Later, the fuel utilization as well as the air utilization can be calculated by equations (4,5), followed by determining the inlet molar flow rates of anode and cathode employing the mass balance equations for each gas component equations (6-20). Then, the cell voltage may be found by Nernst equation (21), also the polarization equations at given operating cell temperature and pressure can be calculated by solving the set of equations (21-29). Finally, the heat and electrical power and efficiency will be determined. More details about the calculation process may be found in [31].

2.3.2. Air compressor

The gas turbine model is comprised of the combined gas turbine and compressor with an interconnecting shaft. The irreversibility effect of the compressor is usually defined by isentropic efficiency. Accordingly, the outlet characteristics $\left(T_8, \bar{h}_8\right)$ of the air compressor can be determined from isentropic efficiency, η_{AC} and $\dot{W}_C$, the used power in the air compressor and as follows [25]:

$$\eta_{AC} = \frac{W_S}{W_a} = \frac{\bar{h}_{8s} - \bar{h}_7}{\bar{h}_8 - \bar{h}_7} \tag{36}$$

$$\frac{T_{8S}}{T_7} = \left(\frac{P_8}{P_7}\right)^{\gamma - 1/\gamma} \tag{37}$$

$$\dot{W}_{AC} = \dot{m}_7\left(\bar{h}_8 - \bar{h}_7\right) \tag{38}$$

where T is temperature, P is pressure, h is specific enthalpy, $\dot{m}$ is mass flow rate ($^{kg}/_{s}$), η_{AC} is the air compressor efficiency and $\bar{h}_{8s}$ is the specific enthalpy of air.

2.3.3. Gas turbine

Then, the gas turbine outlet may be identified by considering the turbine isentropic efficiency, η_{tis} and expansion ratio, P_{rt} equations [25]:

$$\eta_{tis} = \frac{W_a}{W_s} - \frac{\bar{h}_{11} - \bar{h}_{12}}{\bar{h}_{11} - \bar{h}_{12s}} \tag{39}$$

$$P_{rt} = \frac{P_{11}}{P_{12}} \tag{40}$$

where $\bar{h}_{12s}$ is the specific enthalpy of fuel gas.

Further $\dot{W}_T$, the generated power by the turbine, can be determined by the following equations [25]:

$$\dot{W}_T = \sum_i \left(\dot{m}_{11}\bar{h}_{11}\right)_{in} - \sum_i \left(\dot{m}_{12}\bar{h}_{12}\right)_{out} \tag{41}$$

Also, the net power output of the gas turbine, $\dot{W}_{GT}$ can be written as:

$$\dot{W}_{GT} = \left(\dot{W}_T - \dot{W_{AC}}\right)\mu_m \cdot \mu_g \tag{42}$$

where μ_m refers to the mechanical efficiency and μ_g indicates generator efficiencies which are assumed 0.80 and 0.98, respectively. [25].

2.3.4. Combustion chamber

The exhausted fuel from the anode side of the SOFC and the off-air from the cathode side are introduced to a combustor in order to make the unreacted gases to be burnt completely for the heat recovery [30].

The combustion equation of the combustion chamber is as follows [30]:

$$\begin{aligned} CH_4 + X_{O_2}^0 O_2 + X_{N_2}^0 N_2 + X_{CO_2}^0 CO_2 + X_{H_2O}^0 H_2O \\ \rightarrow \left(f + X_{CO_2}^0\right)CO_2 + \left(2f + X_{H_2O}^0\right)H_2O + \left(X_{O_2}^0 - 2f\right)O_2 + X_{N_2}^0 N_2 \end{aligned} \tag{43}$$

where, f is the molar ratio of fuel to air.

Also, the energy balance of the combustor is expressed as [30]:

$$\sum_{i=1}^{6} m_i^{in}\left(\Delta H_f^0 + \int_{298}^{T_{in}} C_p dT\right) = \sum_{i=1}^{4} m_i^{out}\left(\Delta H_f^0 + \int_{298}^{T_{out}} C_p dT\right) \tag{44}$$

It should be noted that the adiabatic combustion temperature may be calculated by equation (44).

2.3.5. Heat recovery steam generator (HRSG)

The HRSG is used to recover energy from turbine exhaust gas as well as to generate some auxiliary steam to be utilized in an internal reformer where water is pumped to the HRSG. The steam flow rate generated by the HRSG, $\dot{m}_s$, may be determined by considering the following equations simultaneously [32]:

$$\dot{m}_g = \dot{m}_a + \dot{m}_f \tag{45}$$

$$\dot{m}_s(h_3 - h_8) = \dot{m}_g(h_{13} - h_{14}) \tag{46}$$

$$\dot{m}_s(h_3 - h_{17P}) = \dot{m}_g(h_{13} - h_{14P}) \tag{47}$$

$$P_0 = P_{13}(1 - \Delta P_{HRSG}) \tag{48}$$

where s represents to steam and g implies gas.

2.3.6. Heat exchangers

The outlet temperature of the air flow that leaves the air preheaters, i.e. T_{13} and T_4, may be calculated by solving the air preheater effectiveness, ε_{APH}, as follows [30]:

$$\varepsilon_{APH1} = \frac{T_{13} - T_8}{T_{12} - T_8} \tag{49}$$

$$\varepsilon_{APH2} = \frac{T_4 - T_2}{T_{14} - T_2} \tag{50}$$

The energy conservation equation for the air preheater may be rearranged as [30]:

$$\dot{m}_8(h_{13} - h_8) = \dot{m}_{12}(h_{12} - h_{13})\varepsilon_{APH1} \tag{51}$$

$$\dot{m}_2(h_4 - h_2) = \dot{m}_{14}(h_{14} - h_4)\varepsilon_{APH2} \tag{52}$$

2.3.7. Fuel compressor

The isentropic efficiency and work of the fuel compressor can be determined as follows [26]:

$$\eta_{FC} = \frac{W_S}{W_a} = \frac{\bar{h}_{2s} - \bar{h}_1}{\bar{h}_2 - \bar{h}_1} \tag{53}$$

$$\dot{W}_{FC} = \dot{m}_f\left(\bar{h}_2 - \bar{h}_1\right) \tag{54}$$

Where $\boldsymbol{\eta_{FC}}$ refers to the mechanical efficiency of fuel compressor, assumed to be 0.78.

2.3.8. Water pump

The isentropic efficiency and work of the water pump can be calculated as [26]:

$$\eta_{wp} = \frac{\bar{h}_{17s} - \bar{h}_{16}}{\bar{h}_{17} - \bar{h}_{16}} \tag{55}$$

$$\dot{W}_{WP} = \dot{m}_W\left(\bar{h}_{17} - \bar{h}_{16}\right) \tag{56}$$

2.3.9. Power and efficiency

The total energy efficiency and net power output of the proposed hybrid system including the SOFC and GT hybrid cycle is determined as following [30]:

$$\dot{W}_{net} = (\dot{W}_{SOFC} + \dot{W}_{GT} - \dot{W}_{FC} - \dot{W}_{WP}) \tag{57}$$

$$\dot{Q}_{tot} = (\dot{m}_f \cdot U_f \cdot LHV) \tag{58}$$

$$\eta_{HS} = \frac{\dot{W}_{net}}{\dot{Q}_{tot}} \tag{59}$$

2.4 Simulation and validation

The proposed model developed in the preceding sections is employed to simulate and assess the performance of the SOFC-GT hybrid system. The nominal model inlet parameters of the studied SOFC-GT CHP system are summarized in Table 2 while more details may be found in [25, 28]. In

Table 3, in order to indicate the model validation and accuracy, some simulation results of the proposed model (SOFC-GT) are compared to the existing studies [28]. It is observed that the presented results reasonably agree with the counterparts in literature.

3. OPTIMIZATION METHODS

To obtain the optimum solution for both maximum efficiency and output power of the SOFC-GT system, a mathematical method is required. Generally, two categories of optimization methods are discussed in literature [33]; the first category is the classical optimization methods like the linear programming (LP); while the next type is the heuristic method. Since finding the optimum solution for the integrated SOFC-GT system is defined under nonlinear categories and determining the optimal values with conventional methods is slightly complicated, the heuristic method has been implemented in this work. Both the GA and the PSO are employed in this optimization problem. Since both optimization approaches are supposed to determine the optimal solutions to a given objective function while employing different procedures, it is essential and helpful to compare their performance.

3.1. Multi-objective optimization

Recently, multi-objective optimization problems have been extensively studied, and various viable solutions have been found in the literature [2, 3, 6, 9, 22, 34]. Multi-objective problem appears virtually in different fields and has been widely applied in a variety of contexts such as, designing aircraft control systems, designing structures, and vehicles, as well as dealing with pollution control and management problems [22].

A multi-objective optimization approach is capable of finding the solution to a problem with numerous objectives simultaneously where such objectives are regularly in conflict with each other, such as the seek for maximum efficiency or maximum power generation and minimum cost at the same time [34].

Although there is no unique correct solution to MOO problems, instead there is a set of solutions whereas one is called the Pareto set. Therefore, decision making is required to select the best answers from the Pareto solutions.

The MOO problem may be demonstrated as [34]:

$$\mathrm{Min}_{x} f(x) = [\, f_1(x), f_2(x), f(x), \dots,\ f_n(x)]^T \qquad (60)$$

Subject to:

$$h_j(x) = 0 \quad j = 1, 2, \dots, n \tag{61}$$

$$g_i(x) \leq 0 \quad i = 1, 2, \dots, m \tag{62}$$

where, $f_n(x)$ refers to the n^{th} objective function, $h(x)$ and $g(x)$ are the equality and inequality constraints, respectively, and x indicates the vector of decision variables.

3.2 The MINSOOP algorithm

Although, there is a vast pool of analytical methods to solve the multi-objective problems, they generally fall into two main categories: the preference-based and the generating methods. Preference-based methods like goal programming are conventional optimization techniques that takes into account the decision maker's preferences, thus distinguish the solution that meets the decision maker's preference perfectly. Generating approaches like the constraint method and the weighting method, have been widely developed to obtain the exact Pareto solution or an estimate of it.

A leading procedure for determining a solution is to consider minimizing one of the objectives while the rest are treated as inequality constraints with a parametric right-hand-side. The problem can be defined as:

$$\text{Minimize } Z_j \tag{63}$$

Subject to:

$$h(x, y) = 0 \tag{64}$$

$$g(x, y) \leq 0 \tag{65}$$

$$Z_k \leq L_k, \quad k = 1 \dots, j-1, j+1, \dots, p; \quad p \geq 2 \tag{66}$$

where Z_j refers to the selected j^{th} objective that requires to be optimized. Solving frequently for various values of L_k selected between the upper bounds, $Z_L(j)$, and lower bounds, $Z_U(j)$, leads to the Pareto set. In this study, the MOO and the Minimization Single Objective Optimization Problem (MINSOOP) are employed to identify the optimal Pareto solutions to given objectives [22].

3.3 Genetic Algorithm

A GA is an adaptive heuristic search algorithm, inspired by the evolutionary ideas of natural selection and genetics that is employed to seek for solving constrained and unconstrained optimization problems and examine solutions to optimization problems [35].

The foremost merit of employing GA is its capability to explore in parallel and using a population of points, which assists it to avoid being trapped in a locally optimal solution. It is essential to use genetic operators such as crossover, mutation and selection at the search onset to achieve better and fitter solutions to eventually end in a single solution. The advantage of using crossover is that it determines how the genetic algorithm merges two individuals to produce a crossover child for the next generation. It is worth mentioning that the mutation specifies the stochastic changes in populations necessary to produce mutation children. Also, the selection step enables selection of parents for the next generation [35]. The GA algorithm procedure is shown in Fig. 2.

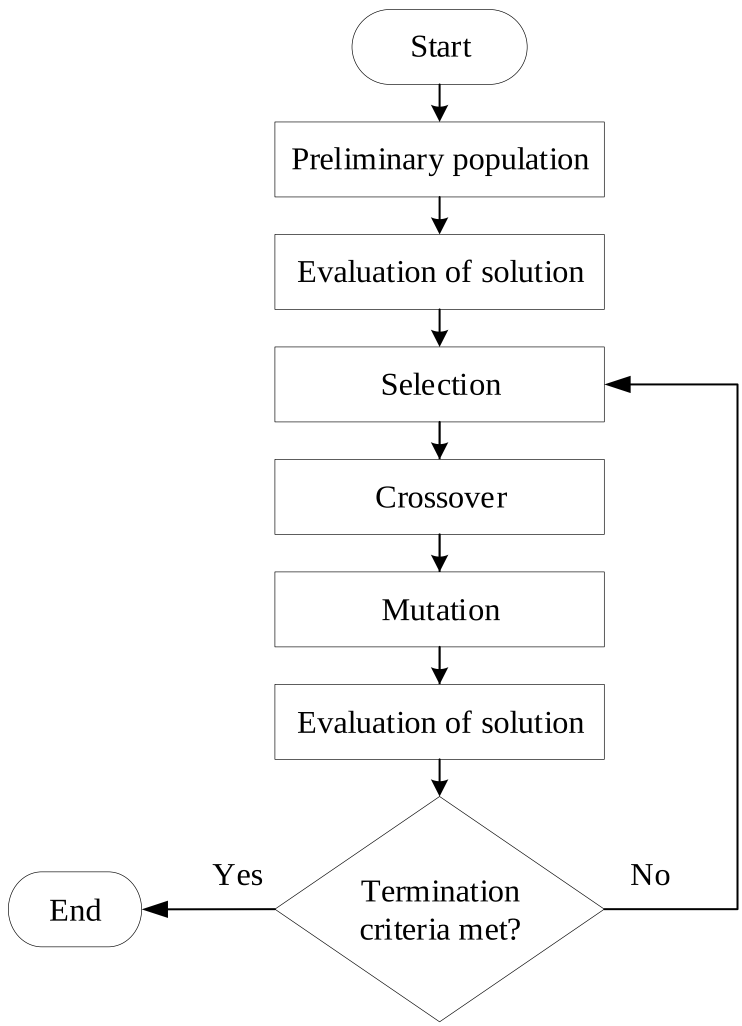

Fig. 2. the GA algorithm procedure.

As illustrated in Fig. 2, the major activity in GA is defining the fitness function that in turn reveals the solution. Then, the genetic algorithm searches for a probabilistic technique to accomplish the final objective function values.

3.4. Particle Swarm Optimization

The PSO optimization technique is built on the movement and intelligence of swarms. Indeed, it is created based on how fish and birds move seeking for food. Any particle demonstrates a possible answer to a problem. The aim of the particles in the PSO is to find a global optimum point in a search space [35].

The PSO model is employed while considering the fitness value, whereas, the particles exhibit the fitness value solutions. Also, other features like the velocity of each particle were considered to determine the direction of particle movement. Interestingly, the particles adjust their directions corresponding to the best fitness value. It is worth noting that position and velocity are the key features of every member in PSO. In this work, the collective location of the swarm and the best location of each distinct particle per time step are calculated. The new search orientation consists of these two orientations as well as the preceding orientation [35]. Here, the best location of an individual particle and all particles for a D dimension search space may be found by equations (67) and (68), respectively.

The PSO algorithm is described as [35]:

$$\vec{P}_1 = C_1(\vec{P}_{i1}, \vec{P}_{i2}, \dots, \vec{P}_{iD}) \tag{67}$$

$$\vec{g} = C_2(g_1, g_2, \dots, g_D) \tag{68}$$

Also, the best location in the surrounding of any individual particle is obtained by the following equation [35]:

$$\vec{n} = (n_{i1}, n_{i2}, \dots, n_{iD}) \tag{69}$$

Particle displacement is found as below after specifying the corresponding velocity [35]:

$$\vec{X}(t) = \vec{X}(t-1) + \vec{V}(t) \tag{70}$$

$$\vec{V}(t) = \vec{V}(t-1) + \vec{F}(t-1) \tag{71}$$

The force inflow to the particle can be examined by [35]:

$$\vec{F}_{i-1} = C_1(\vec{P}_{i-1} - \vec{X}_{i-1}) + C_2(\vec{g}_{i-1} - \vec{X}_{i-1}) \tag{72}$$

where the acceleration coefficients of C_1 refers to cognitive parameter and C_2 denotes the social parameter.

The ultimate correlation of the particle velocity at dimension d with the next iteration can be written as [35]:

$$V_{id}(t) = \omega V_{id}(t-1) + C_1 r_1 \left(\vec{P}_{id}(t-1) - \vec{X}_{id}(t-1)\right) + C_2 r_2 (n_{id}(t-1) - X_{id}(t-1)) \tag{73}$$

It demonstrates the particle velocity i at the global best. The numbers r_1 and r_2 are constants randomly distributes between 0 and 1, and ω is the inertia weight. It plays a crucial role in the PSO convergence quality and speed since it is the deterministic parameter in search behavior of swarms. In order to accelerate the convergence at the local optima, the parameter "X" is employed while it should be noted that it may have adverse effect and prevent the convergence when excessive values are assigned to it. In practice, a value of one is assigned to "X" throughout the learning process while it is gradually and linearly reduced down to zero. An illustrative schematic of PSO algorithm is displayed in Figure 3 [35].

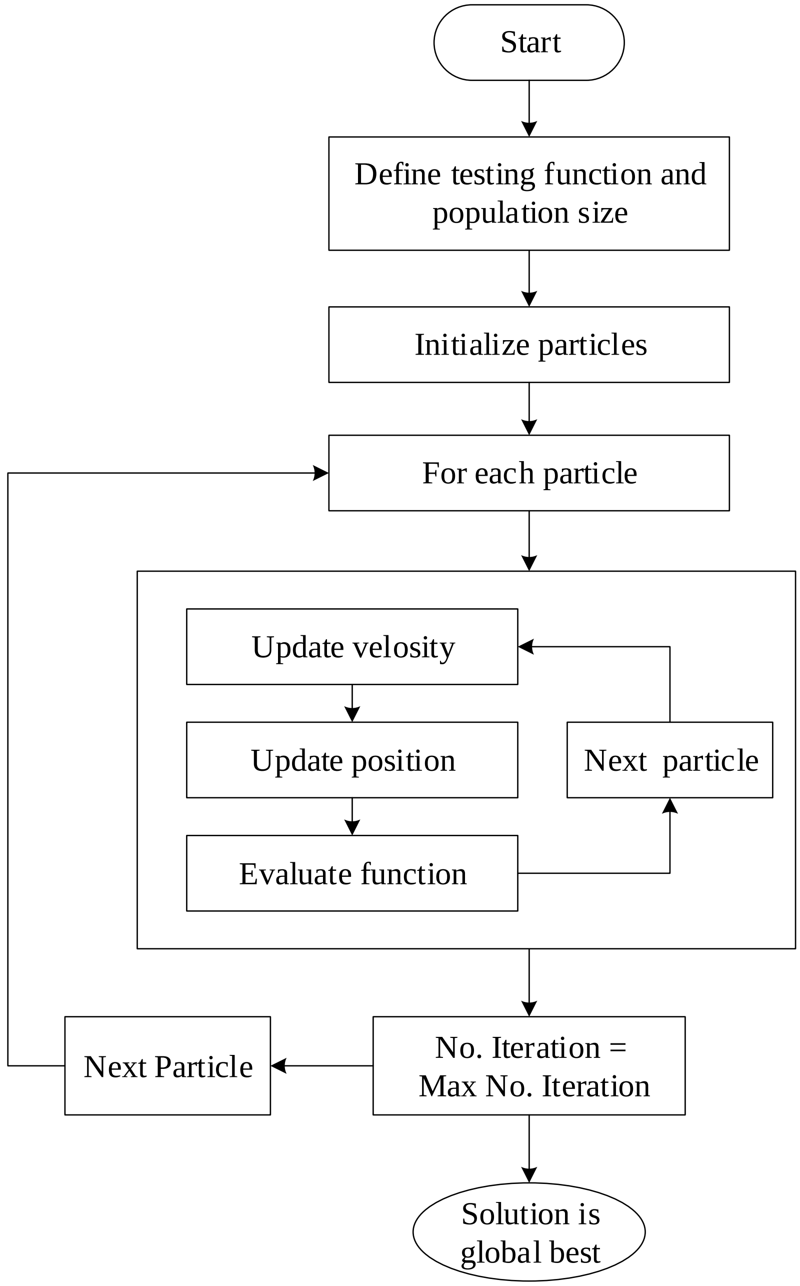

Fig. 3. PSO algorithm procedure

3.5 Objective function formulation

As discussed earlier, current study investigates the optimum operating condition of the SOFC-GT system in terms of maximizing both efficiency and output power simultaneously.

Typically, the efficiency of the SOFC/GT system is reduced significantly as its power output increases. Therefore, the objectives in such problems are in conflict with each other. Hence, MINSOOP approach is employed to form the objective function as follows:

$$\text{Min } \eta_{HS}\left(U_f, rp_{gt}, \dot{m}_{fuel}, r_{sc}\right) = (-1)\frac{(\dot{W}_{SOFC} + \dot{W}_{GT} - \dot{W}_{FC} - \dot{W}_{WP})}{\dot{m}_{fuel} * U_f * LHV} \quad (74)$$

$$\text{Min } \dot{W}_{net}\left(U_f, rp_{gt}, \dot{m}_{fuel}, r_{sc}\right) = (-1)(\dot{W}_{SOFC} + \dot{W}_{GT} - \dot{W}_{FC} - \dot{W}_{WP}) \quad (75)$$

where η_{HS} and $\dot{W}_{net}$ are hybrid system efficiency and the net output power, respectively, U_f is fuel utilization factor, p_{rc} refers to the pressure ratio, $\dot{m}_{fuel}$ is the mass flow rate of fuel at the anode inlet and r_{sc} is the steam to carbon ratio in the internal reformer.

It is worth noting that η_{HS} and $\dot{W}_{net}$ are the objective functions aimed to be maximized. The fitness function is formulated as follows:

$$Z = -w * \eta_{HS} - (1 - w)\dot{W}_{net} \quad (76)$$

To solve the multi-objective problems, the first step is to build a payoff table. A payoff table consists of the single optimization problems, with assigned weight factors of 0 or 1 in order to find the possible ranges of the objectives $Z_U(j)$ (the upper bound), and $Z_L(j)$ (the lower bound) [22].

The contrast in the scales of the parameters of these objective functions is the principal concern of optimization. The value of $\dot{W}_{tot}$ ranges from 42.15 kW to 408 kW, while the value of η_{HS} lies between 0.15 and 0.88. Therefore, solving the problem without employing such conditions, results in looking for the maximum power ignoring the efficiency, no matter what weight factor is assigned to the parameters [34]. To overcome this problem, the parameters are normalized to accomplish the complete trade-off between 0 and 1 value [22] This strategy is defined comprehensively in [36]. Finally, the fitness function is changed as:

$$Z_{Norm} = -w.\left[\frac{\eta_{HS} - 0.15}{0.88 - 0.15}\right] - (1 - w).\left[\frac{\dot{W}_{net} - 42.15}{408 - 42.15}\right] \quad (77)$$

The multi-objective optimization procedure seeks optimum values regarding the given decision variables range. However, MATLAB GA optimization is employed to achieve the optimum solutions and to model the system. PSO algorithm is also developed in MATLAB. As discussed in the previous section, the PSO algorithm principles start from an initial swarm or population and apply a research strategy based on the participation of its Ne particles.

In the PSO procedure, the speed has a pivotal role that leads the search in the promising zones of the solution area. To avoid consuming an extensive computation time, the parameters should be selected within an appropriate boundary. Population size is strongly linked to the search space. In case a very small parameter is selected, the algorithm will probably converge to a local optimum; whereas, if an excessively large population size is assigned, a high computational time would be required. After several examinations, it is found that the best performance of PSO will be accomplished if a population size of nearly 30 is selected, which is within the suggested population size of 30–50 recommended by [37].

The number of PSO swarm members is assumed 30 whose positions and velocities are randomly assigned in the searching domain. Each swarm member has four dimensions, i.e. U_f, p_{rc}, r_{sc} and $\dot{m}_{fuel}$. According to the system limitations, the minimum and maximum values of the four dimensions are presented in Table 4.

In this study, C_1, C_2 are considered to be 2 while r_1, r_2 are in the range of [0, 1]. It should be noted that these are the algorithm inputs related to SOFC-GT hybrid system. In order to apply these limitation parameters, particles that have a position outside of this range will be penalized with a very small-scale value of objective function. Therefore, PSO algorithm does not select such positions as the preferred position. To prevent the local responses and noises in output results, PSO algorithm is iterated three times to select the best response with the optimum objective function as the output. The termination criteria is determined as:

$$\frac{g_{best}^{k} - g_{best}^{k+1}}{g_{best}^{k}} < (e = 10^{-6}) \tag{78}$$

3.6 Solution methodology

In this work, we have employed a solution methodology that leads to the optimal operation conditions and the set of optimal solutions for the objective functions as shown in Fig. 4. It should be noted that both technical and optimization factors are taken into consideration as illustrated in Fig. 4, namely the technical model and the multi-objective optimization model including both PSO and GA algorithms. In order to solve the technical model, decision variables and constant parameters are selected followed by modelling the fuel compressor, fuel processing, SOFC, GT, HRSG, and the energy balance. Later, power and efficiency as the dependent variables are passed to the MOO model as objective functions to demonstrate two distinct Pareto curves using GA and PSO as solution procedures.

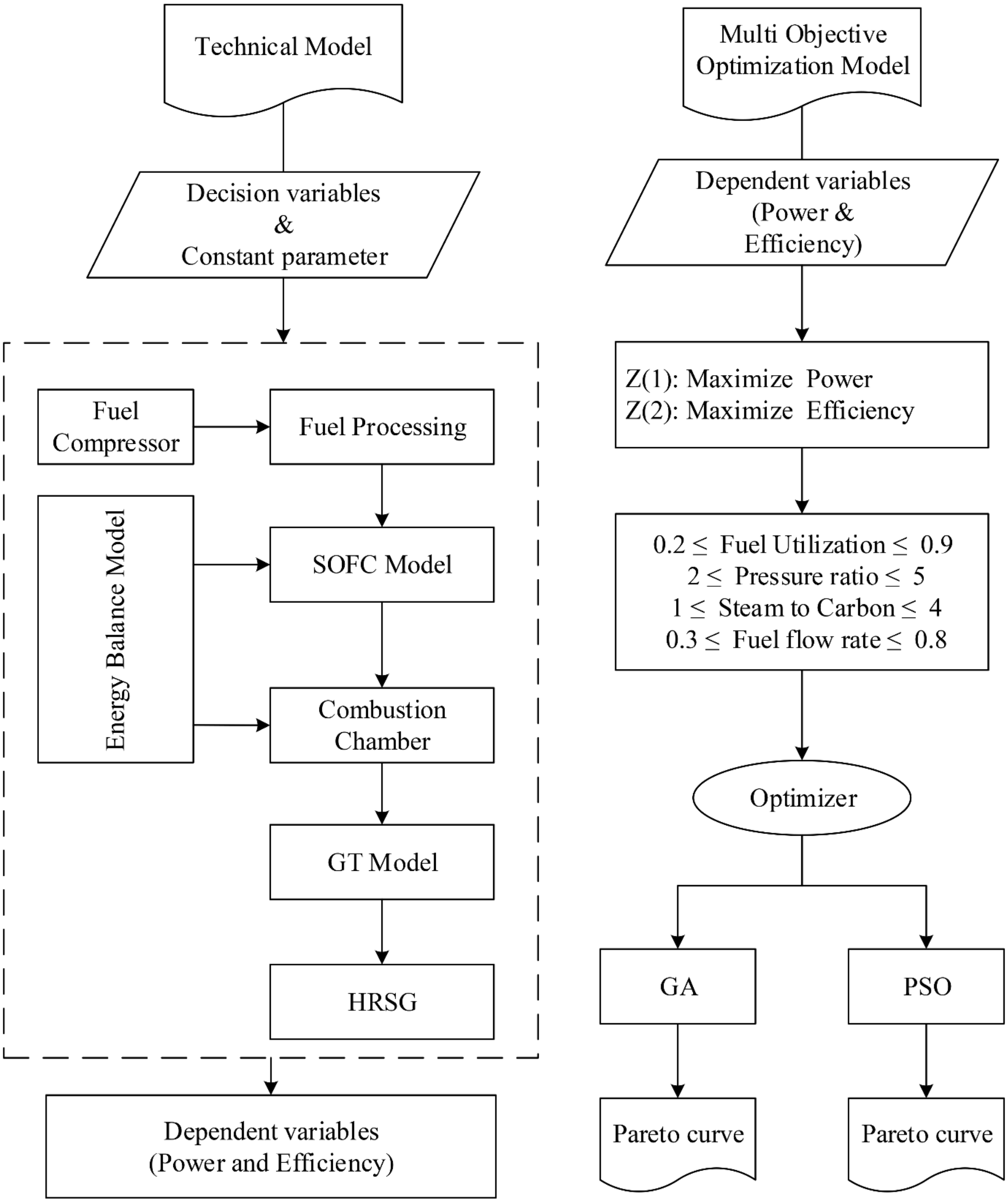

Fig. 4. Solution methodology applied on MOO problem of proposed integrated system

4. RESULTS AND DISCUSSION

At first, the modeling results are demonstrated to show the impact of the operating parameters. Then, two intelligent algorithms are compared for optimizing SOFC-GT hybrid system.

4.1. Modeling results

Since the net power generation and the energy efficiency of the system are a function of different parameters, the influence of some vital parameters on the integrated SOFC-GT system is illustrated later.

The influence of the pressure ratio on the performance of SOFC-GT hybrid power system is shown in Fig. 5. The output power and efficiency of hybrid system are small at lower P_{rc} values. It is observed that improving the pressure ratio significantly enhances both the efficiency and power until it reaches some point after which pressure ratio rise only contributes to a slight enhancement. This is mainly due to the increase of the energy consumption of compressor, which consequently decreases the net power generation of gas turbine. Thus, P_{rc} range from 2 to 5 is selected and studied later, since the best improvement is experienced in this range, i.e. the overall power increases from 220 kW to 350 kW, also efficiency improves from 61% to 82%.

As indicated, the compressor pressure ratio has a remarkable outcome on both the net system power and efficiency, and can increase the compressor work. It means that the compressor pressure ratio can be optimized to improve the overall system performance.

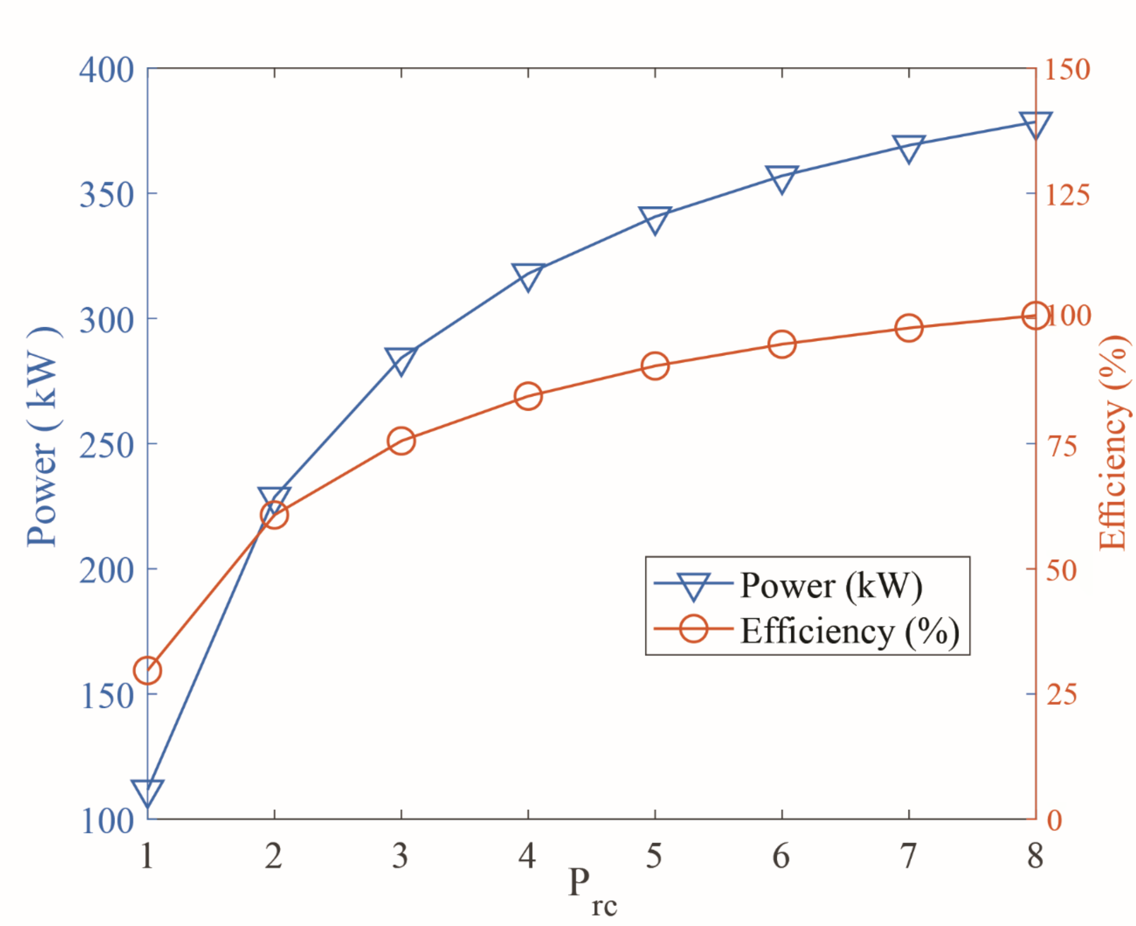

Fig. 5. The effect of pressure ratio on the system efficiency and output power.

The U_f is an influential parameter on the power and energy efficiency of the system which is defined as the ratio of hydrogen amount participated in the electrochemical reaction in the SOFC to the amount of supplied fuel.

Fig. 6 demonstrates the effect of U_f on the system net output power. The power generated by the SOFC increases as U_f increases. The main reason is, while the amount of hydrogen consumed in the SOFC increases, the temperature at which the SOFC operates also increases, thus the system net output power is improved.

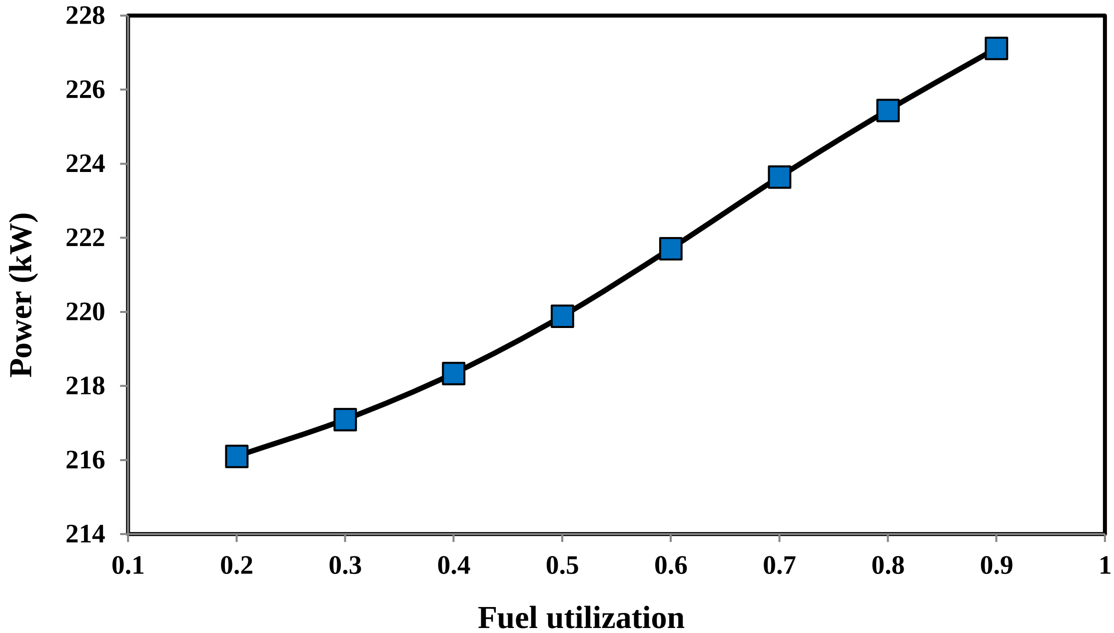

Fig. 6. The impact of U_f on the SOFC-GT system output power.

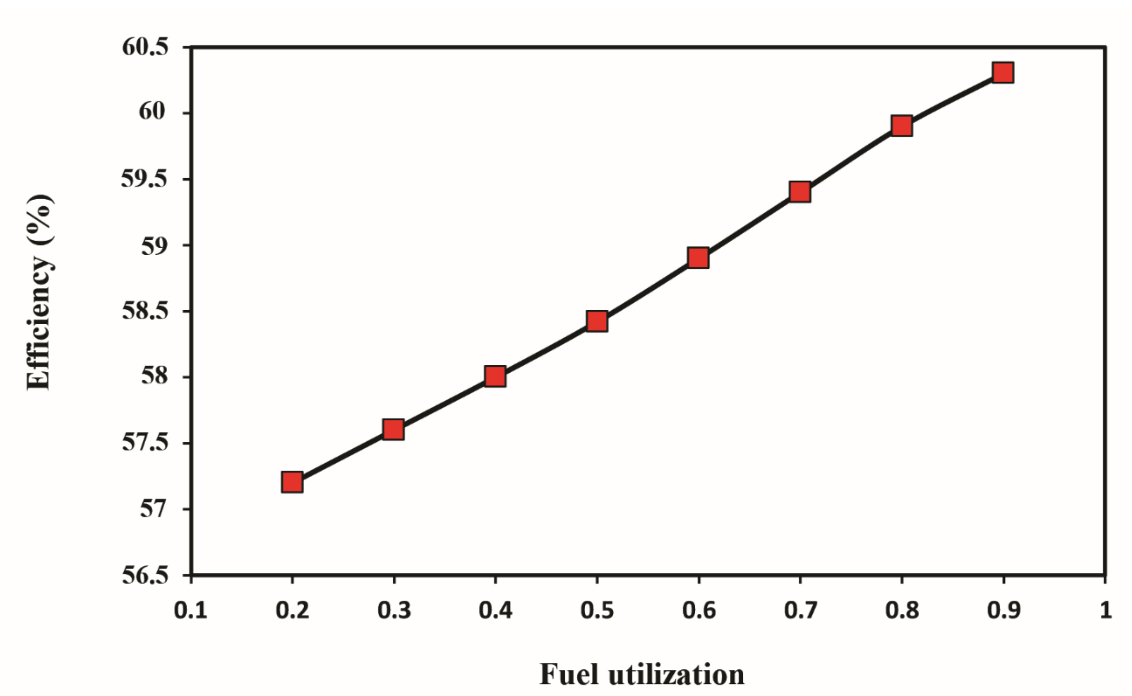

Fig. 7. The impact of U_f on the SOFC-GT system efficiency.

The impact of U_f on the system energy efficiency is presented in Fig. 7. The efficiency enhancement trend is similar to Fig. 6, while efficiency undergoes a slightly linear improvement as fuel utilization increases. As expected, when the power increases the system energy efficiency is consequently improved.

Comparing Figs. 6 & 7, it is found out that at any given condition, operation at higher U_f results in achieving enhanced system power and energy efficiency. However, employing higher U_f have a straight effect on the power consumption by the fuel blower. Accordingly, a tradeoff between generating the additional output power and the consumption of auxiliary power of blowers should be considered. Eventually, the results confirm that this an excellent choice as one of the decision variables of the system.

4.2. Optimization results

A proper comparison between the PSO and the GA is performed for maximizing the net output power and the energy efficiency of the SOFC-GT system. For accomplishing this target, the MOO algorithm is employed. The curves of the power and the efficiency are plotted over different number of convergence iterations as shown in Fig. 8 and Fig. 9, respectively. The same population size (P = 30) is considered in both figures.

As it is observed, the PSO algorithm has a faster convergence compared to the GA. The best output power for PSO is achieved at 432.8 s, while this happens in 620.4 s for GA. This reveals that the PSO approach reaches the optimum solution 187.6 s faster than the GA when using the same population size.

This is mainly because PSO does not possess genetic operators like mutation; consequently, particles will be updated according to the internal velocity. Due to their memory as well as unique information sharing mechanism where only the best particle reveals the information to others, the PSO excels to find the best solution more efficiently in comparison to GA. Moreover, PSO achieves a better solution with fewer number of iterations. In this study, the best solution of power is achieved by 39 convergence iterations when employing PSO, while GA reaches the best solution in 56 convergence iterations.

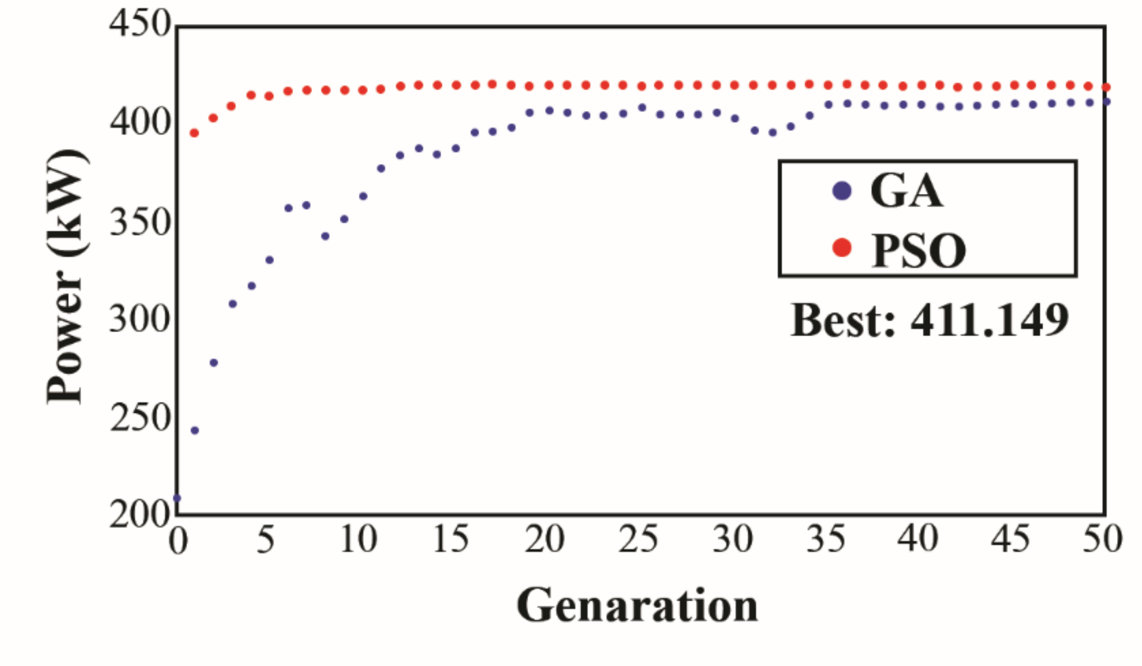

Fig. 8. The SOFC/GT system output power over generations of both GA and PSO algorithms.

As shown in Fig. 9, similar to the optimization of the system power, the PSO algorithm exhibits better performance on the efficiency optimization. The PSO algorithm indicates faster convergence where it reaches to the best efficiency at 507.2 s in comparison to GA obtaining the best efficiency at 586.15 s. Hence, PSO is found to reach the optimum solution 78.95 s faster than GA.

These results are compatible with findings from references [37, 38]. Regarding an evolutionary viewpoint, the performance of the PSO is significantly better than the GA such that it takes fewer generations for PSO to succeed at its final parameter values compared to GA. Moreover, it is found that the PSO algorithm reaches to the best solution at approximately 20 generations for energy efficiency optimization. This is mainly since the PSO algorithm is comprised of particles that are randomly initialized and influenced by their best past location. The particles are updated by the internal velocity and hold a memory which makes it faster than GA.

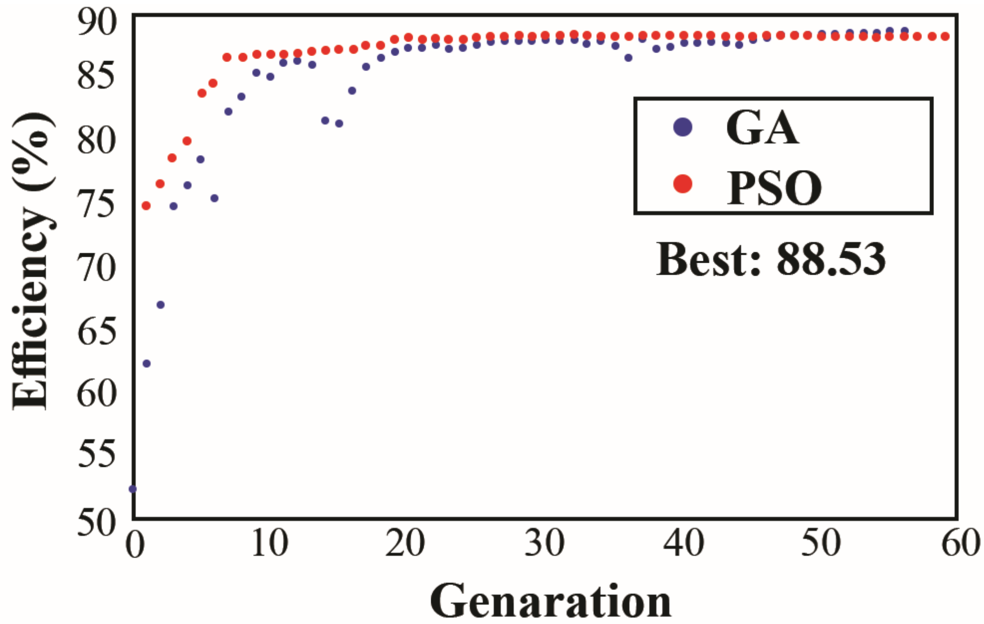

Fig. 9. The SOFC/GT system efficiency over generations of both GA and PSO algorithms.

The output power optimization versus efficiency objective function considering the PSO and GA procedures are shown in Fig. 10 and Fig. 11, respectively. Pareto front diagrams are generated for the purpose of trade-off analysis between energy efficiency and the net output power. As already anticipated, the conflict between the examined objective functions is obvious in Fig. 10. It is observed that improving the power in the set leads to hindering the efficiency.

In analyzing the energy efficiency and the net output power alternatives, decision makers often seek to know the optimum solution between two objective functions. For instance, if it is aimed to generate the maximum power, i.e. 419.2 kW, the energy efficiency will be equal to 58%. In contrast, if the highest energy efficiency is targeted, i.e. 88%, the net output power will be about 210 kW. Therefore, Pareto optimality allows decision makers to choose between target functions in accordance with the optimal performance requirements.

Since the diagram slope changes drastically above the energy efficiency of 74% and below the net output power of 360 kW, the best optimum solution in terms of both the energy efficiency and the net output power is determined in the specified region marked in Figure. 10. It is observed from the Pareto optimality that for producing 402 kW power, the energy efficiency is equal to 67% whereas the energy efficiency improves approximately by 10 % and reaches up to 73.7% when the net output power reaches to 364kW, that is equal to 9.4% drop in power generation.

Alternatively, if the energy efficiency of 84% is intended, the power generation will be equal to 270 kW. This means if the efficiency improves by 25% the power generation will be dropped by 32.8%.

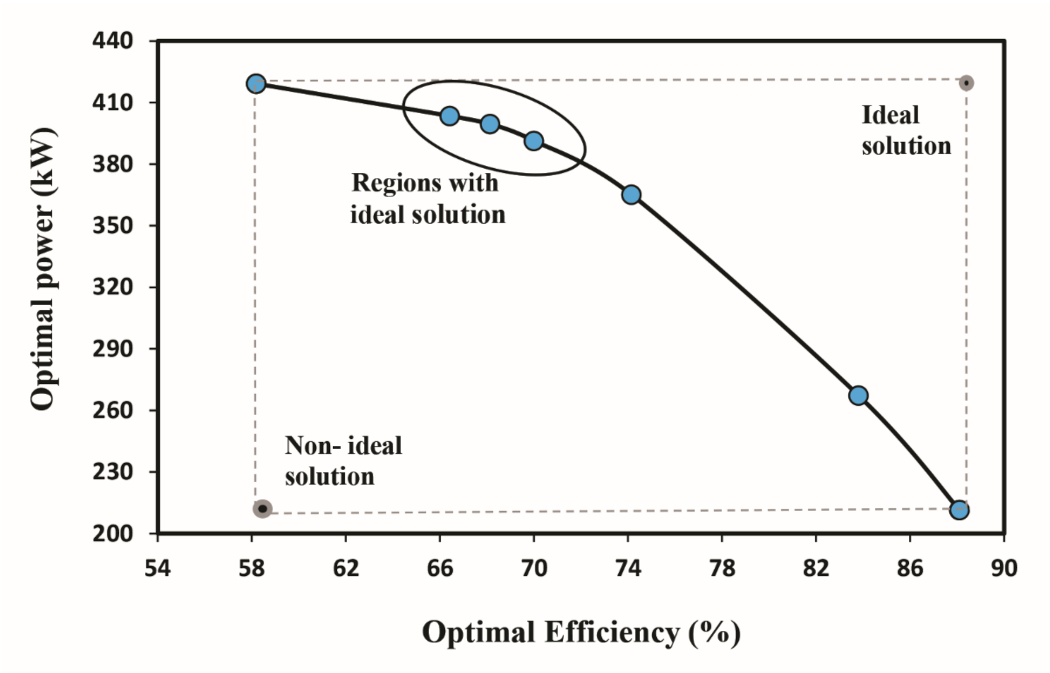

Fig. 10. The Pareto optimality diagram of the system output power and efficiency of PSO algorithm.

The changes in the decision variables in regard to a variety of weighting factors by the GA approach is shown in Fig. 11. In the Pareto front, point A (W=0) indicates the maximum power generation, 410.5 kW, at 64% efficiency. As it is clear, by increasing the weighting factor (W) or enhancing the importance of the energy efficiency, less power is generated while the efficiency will be enhanced gradually. On the other hand, point B (W=1) refers to the maximum efficiency of 88% for a 210-kW power generation. Based on this trade off of the Pareto optimality, the decision makers are able to adjust the efficiency in respect to the expected power generation and vice versa.

By comparing these two Pareto front diagrams, it can be seen that in the GA optimization method, the maximum net output power of 410 kW is achieved while the energy efficiency is 64%, whereas in the PSO method the maximum net output power of 419.2kW is obtained at the energy efficiency of 58.9%.

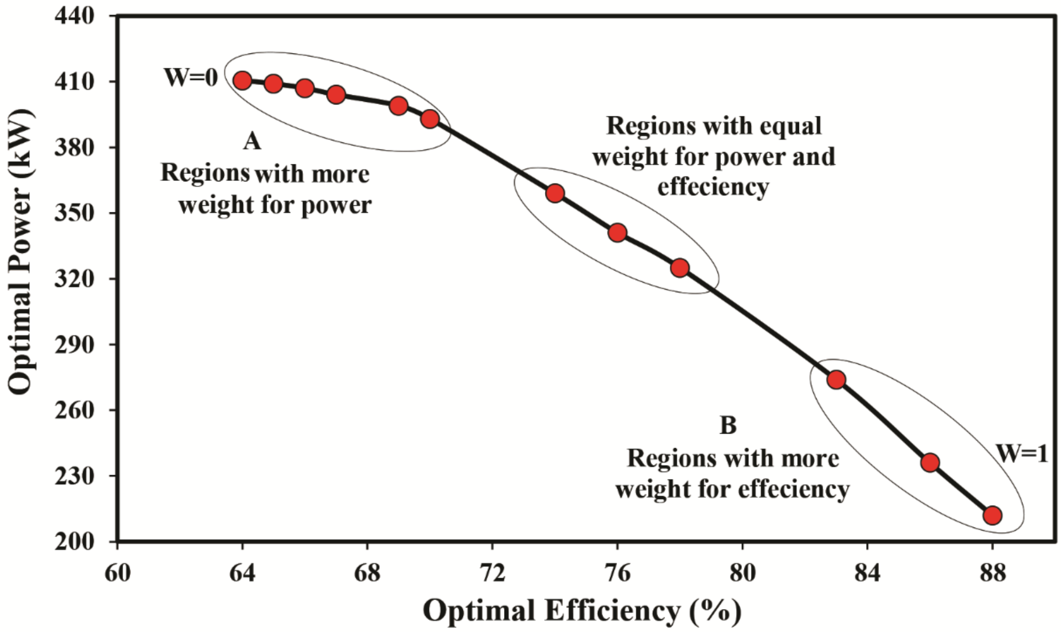

Fig. 11. The Pareto optimality diagram of the system output power and efficiency of GA algorithm.

To make a ready comparison, the parameters of both algorithms are presented in Table 5. Moreover, the best outcomes of both proposed algorithms are compared and briefly indicated in

Table *6*. It is found that the best solution achieved by the PSO method is obtained when the energy efficiency and the net output power is 88.2% and 419.2 kW, respectively. Also, the GA optimization method concludes 88 % and 410.5 kW for the energy efficiency and net output power, respectively. The PSO not only provides a better speed response compared to the GA in terms of computational results, but also yields a better energy efficiency in terms of computational time minimization.

It is figured out that the impact of U_f on improving the energy efficiency is stronger than on the net output power. The optimum net output power in the PSO method is achieved by the U_f of 0.79 while the GA reaches to the optimum solutions by a U_f of 0.85.

The U_f is a pivotal parameter which is remarkably associated with the effectiveness of SOFCs and reflects the efficiency of the integrated systems. Higher utilization factor is reached when a larger portion of the inlet fuel reacts in SOFC, and a smaller portion is introduced into the combustion chamber of the GT. The U_f enhancement means more fuel is involved in the electrochemical reactions, thus in the anode outlet, the percentage of CO_2 will be increased in comparison to H_2 and CO. Consequently, the power generation by the GT cycle will be decreased. On the other hand, as U_f is boosted, the electrochemical reaction rates increase, hence the electrical power output generated by the SOFC is improved. As expected, the contribution of the SOFC to the overall output power of 419 kW increases as U_f increases.

Therefore, in order to provide a reasonable energy efficiency and net output power, the fuel U_f is required to be maintained between 0.79 and 0.85 according to this simulation which agrees with commercial SOFC U_f values in the market [39]. Increasing $\dot{m}_{fuel}$ will increase the current density and voltage in the SOFC that results in more power production. In contrast, the higher fuel consumption has a negative effect on the energy efficiency. Also, steam offered the best performance as reforming agent for methane according to the results observed from the simulation and both optimization methods.

In particular, comparing these results with the previous studies, it is worth pointing out that the resultant system energy efficiency in this study is significantly higher compared to other studies [40]. This is not only due to the particular optimization procedure but also may originate from the fact that the isentropic efficiencies of the compressor and turbine in the GT cycle are considered higher than [40].

Also, the present work employs the individual layout and components such as fuel compressor and heat exchangers to increase the operating pressure and temperature of the system. Increasing the operating temperature in SOFC leads to the increase of the voltage thus improvement of the energy efficiency as well as the net output power of the system. At higher operating temperature, the system generates more power. The reason is, as a result of higher operating temperature, speed of reactions is increased and less voltage drop occurs in the SOFC that leads to higher production voltages, therefore, more power generation.

Besides, as temperature is increased, the less quantity of air is required to react. So, the lower $\dot{m}_{air}$ is entered into the system. Since the compressor power consumption is directly proportional to the inlet $\dot{m}_{air}$, the compressor also consumes less power. The cumulative effect of increasing the voltage and reducing the power consumption of the compressor is the enhancement of the power generation of the system. In addition, as the system operating pressure increases, the voltage drops. As a result, the concentration polarization will be decreased, consequently, the system net output power will be enhanced.

5. CONCLUSIONS

In this paper, to simultaneously enhance the energy efficiency and the net output power, an integrated SOFC-GT system is studied by employment of two evolutionary multi-objective optimization algorithms. The optimum operating conditions of the integrated SOFC-GT system, i.e. fuel utilization factor, fuel mass flow rate, pressure ratio and steam to carbon ratio, are determined that suggests a significant performance improvement. This enhancement results from the heat recovery of the exhaust gases of SOFC followed by preheating and substituting the fuel from methane to hydrogen. Pareto curves are employed to find the desired power output at the maximum efficiency with refence to both PSO and GA approaches.

The GA and the PSO methods were applied to the system and the results were compared. The findings indicate that both the GA and the PSO can be considered in the MOO models. Although, the two algorithms nearly exhibit similar performance, in terms of computational effort, the PSO approach is faster and more efficient. The PSO appears to require fewer generations to achieve its ultimate parameter values in comparison to the GA algorithm under the examined conditions. In addition, PSO requires a smaller number of function evaluations. It should be noted that it takes a short time for both algorithms to obtain their results. In terms of the accuracy of the model parameters, the GA matches more closely to the pre-existing values. Hence, it is concluded from the current comparison that the PSO algorithm is more suitable for the SOFC-GT MOO problem. The key findings of this paper are:

- By changing P_{rc} from 2 to 5, the overall electrical power generation and the energy efficiency is increased from 220 kW to 350 kW and from 61% to 82%, respectively.
- By increasing the U_f from 0.2 to 0.9, the electrical power generation and the system energy efficiency increases from 216 to 227 kW and from 57.2% to 60.2%, respectively.
- In comparison between GA and PSO algorithms in terms of convergence speed, PSO is preferable since it reaches the optimum solution 187.6 s for the output power and 78.95 s faster for the efficiency calculations.

- The results of PSO algorithm show that for 402 kW electrical power generation, the energy efficiency is 67%. However, by improving the energy efficiency up to 73.7%, the net output power reaches to 364 kW, that is equal to 9.4% less power production.
- The best results of PSO algorithms demonstrate energy efficiency and net output power of 88.2% and 419.2 kW, respectively, while similar metrics for the GA yield 88 % and 410.5 kW, respectively.

This approach presents a scalable method that can be easily applied to other energy systems. However, some recommendations for the future research in this field are:

- Integration of the absorption chiller to the exhaust gas of HRSG via a heat exchanger to exploit the exhaust energy more efficiently for the cooling purposes.
- Production of hydrogen (as a clean gas with high heating value) by using the generated steam from HRSG in a Cu-Cl or gas reformer.
- Optimization of this cycle with respect to other target functions that considers the other aspects of the system such as exergy, economic and exergo-environmental analyses to maximize the exergy efficiency and minimize the air pollution production, net present value (NPV) and payback period (PP).
- Incorporation of another green system such as a solar energy system, e.g., Heliostat Solar Receiver, or Parabolic Through Collector, to reduce the fuel consumption in the proposed layout.

REFERENCES

[1] Zhao Y, Shah N, Brandon N. Comparison between two optimization strategies for solid oxide fuel cell–gas turbine hybrid cycles. international journal of hydrogen energy. 2011;36(16):10235-46.

[2] Roshandel R, Behzadi Forough A. Two strategies for multi-objective optimisation of solid oxide fuel cell stacks. International Journal of Sustainable Energy. 2014;33(4):854-68.

[3] Khani L, Mehr AS, Yari M, Mahmoudi S. Multi-objective optimization of an indirectly integrated solid oxide fuel cell-gas turbine cogeneration system. International Journal of Hydrogen Energy. 2016;41(46):21470-88.

[4] Reyhani HA, Meratizaman M, Ebrahimi A, Pourali O, Amidpour M. Thermodynamic and economic optimization of SOFC-GT and its cogeneration opportunities using generated syngas from heavy fuel oil gasification. Energy. 2016;107:141-64.

[5] Hines R, Hajilounezhad T, Love-Baker C, Koerner G, Maschmann MR. Growth and Mechanics of Heterogeneous, 3D Carbon Nanotube Forest Microstructures Formed by Sequential Selective-Area Synthesis. ACS Applied Materials & Interfaces. 2020;12(15):17893-900.

[6] Sharma S, Maréchal F. Robust Multi-Objective Optimization of Solid Oxide Fuel Cell–Gas Turbine Hybrid Cycle and Uncertainty Analysis. Journal of Electrochemical Energy Conversion and Storage. 2018;15(4):041007--9.

[7] Zhao Y, Shah N, Brandon N. The Development and Application of a Novel Optimisation Strategy for Solid Oxide Fuel Cell-Gas Turbine Hybrid Cycles. Fuel Cells. 2010;10(1):181-93.
[8] Brown J, Hajilounezhad T, Dee NT, Kim S, Hart AJ, Maschmann MR. Delamination Mechanics of Carbon Nanotube Micropillars. ACS Applied Materials & Interfaces. 2019;11(38):35221-7.
[9] Burer M, Tanaka K, Favrat D, Yamada K. Multi-criteria optimization of a district cogeneration plant integrating a solid oxide fuel cell–gas turbine combined cycle, heat pumps and chillers. Energy. 2003;28(6):497-518.
[10] Mobadersani F, Safari H, Hajilounezhad T, Kahroba P. The Effect of Fluid Properties on the Operation of Thermal Bubble jet. arXiv preprint arXiv:191007901. 2019.
[11] Zhang X, Chan S, Li G, Ho H, Li J, Feng Z. A review of integration strategies for solid oxide fuel cells. Journal of Power Sources. 2010;195(3):685-702.
[12] Burbank Jr W, Witmer D, Holcomb F. Model of a novel pressurized solid oxide fuel cell gas turbine hybrid engine. Journal of Power Sources. 2009;193(2):656-64.
[13] Hajilounezhad T, Ajiboye DM, Maschmann MR. Evaluating the Forces Generated During Carbon Nanotube Forest Growth and Self-Assembly. Materialia. 2019:100371.
[14] Gengo T, Ando Y, Kabata T. Development of 200 kW class SOFC combined cycle system and future view. Technical Review Mitsubishi Heavy Industries, Ltd. 2008;45.
[15] Hajilounezhad T, Oraibi ZA, Surya R, Bunyak F, Maschmann MR, Calyam P, et al. Exploration of Carbon Nanotube Forest Synthesis-Structure Relationships Using Physics-Based Simulation and Machine Learning. 2020.
[16] Buonomano A, Calise F, d'Accadia MD, Palombo A, Vicidomini M. Hybrid solid oxide fuel cells–gas turbine systems for combined heat and power: a review. Applied Energy. 2015;156:32-85.
[17] Calise F, Palombo A, Vanoli L. Design and partial load exergy analysis of hybrid SOFC–GT power plant. Journal of power sources. 2006;158(1):225-44.
[18] Hajilounezhad T, Maschmann MR. Numerical Investigation of Internal Forces During Carbon Nanotube Forest Self-Assembly. Conference Numerical Investigation of Internal Forces During Carbon Nanotube Forest Self-Assembly. American Society of Mechanical Engineers, p. V002T02A88-VT02A88.
[19] Lundberg W, Veyo S, Moeckel M. A high-efficiency solid oxide fuel cell hybrid power system using the Mercury 50 advanced turbine systems gas turbine. Journal of Engineering for Gas Turbines and Power. 2003;125(1):51-8.
[20] Hajilounezhad T. Numerical evaluation of dry-cooling towers interaction in different arrangement. 2019.
[21] Autissier N, Palazzi F, Maréchal F, Van Herle J, Favrat D. Thermo-economic optimization of a solid oxide fuel cell, gas turbine hybrid system. Journal of fuel cell science and technology. 2007;4(2):123-9.
[22] Subramanyan K, Diwekar UM, Goyal A. Multi-objective optimization for hybrid fuel cells power system under uncertainty. Journal of power sources. 2004;132(1-2):99-112.
[23] Ramadhani F, Hussain M, Mokhlis H, Hajimolana S. Optimization strategies for Solid Oxide Fuel Cell (SOFC) application: A literature survey. Renewable and Sustainable Energy Reviews. 2017;76:460-84.
[24] Konak A, Coit DW, Smith AE. Multi-objective optimization using genetic algorithms: A tutorial. Reliability Engineering & System Safety. 2006;91(9):992-1007.
[25] Akkaya AV, Sahin B, Erdem HH. An analysis of SOFC/GT CHP system based on exergetic performance criteria. International Journal of Hydrogen Energy. 2008;33(10):2566-77.
[26] Forough AB, Roshandel R. Design and operation optimization of an internal reforming solid oxide fuel cell integrated system based on multi objective approach. Applied Thermal Engineering. 2017;114:561-72.
[27] George RA. Status of tubular SOFC field unit demonstrations. Journal of Power Sources. 2000;86(1-2):134-9.
[28] Akkaya AV. Electrochemical model for performance analysis of a tubular SOFC. International Journal of Energy Research. 2007;31(1):79-98.
[29] Chitsaz A, Mahmoudi SMS, Rosen MA. Greenhouse gas emission and exergy analyses of an integrated trigeneration system driven by a solid oxide fuel cell. Applied Thermal Engineering. 2015;86:81-90.
[30] Shamoushaki M, Ehyaei M, Ghanatir F. Exergy, economic and environmental analysis and multi-objective optimization of a SOFC-GT power plant. Energy. 2017;134:515-31.
[31] Safari S, Hajilounezhad T, Aliehyaei M. Multi-Objective Optimization of Solid Oxide Fuel Cell/GT Combined Heat and Power System: A comparison between Particle Swarm and Genetic Algorithms. 2020.
[32] Yazdi BA, Yazdi BA, Ehyaei MA, Ahmadi A. Optimization of micro combined heat and power gas turbine by genetic algorithm. Thermal Science. 2015;19(1):207-18.
[33] Calise F, d'Accadia MD, Vanoli L, von Spakovsky MR. Full load synthesis/design optimization of a hybrid SOFC–GT power plant. Energy. 2007;32(4):446-58.
[34] Mert SO, Özçelik Z, Özçelik Y, Dinçer I. Multi-objective optimization of a vehicular PEM fuel cell system. Applied Thermal Engineering. 2011;31(13):2171-6.

[35] Sadeghzadeh H, Ehyaei M, Rosen M. Techno-economic optimization of a shell and tube heat exchanger by genetic and particle swarm algorithms. Energy Conversion and Management. 2015;93:84-91.
[36] Marler RT, Arora JS. Survey of multi-objective optimization methods for engineering. Structural and multidisciplinary optimization. 2004;26(6):369-95.
[37] López PR, González MG, Reyes NR, Jurado F. Optimization of biomass fuelled systems for distributed power generation using particle swarm optimization. Electric Power Systems Research. 2008;78(8):1448-55.
[38] Panda S, Padhy NP. Comparison of particle swarm optimization and genetic algorithm for FACTS-based controller design. Applied soft computing. 2008;8(4):1418-27.
[39] Braun RJ. Optimal design and operation of solid oxide fuel cell systems for small-scale stationary applications. 2002.
[40] Meng Q, Han J, Kong L, Liu H, Zhang T, Yu Z. Thermodynamic analysis of combined power generation system based on SOFC/GT and transcritical carbon dioxide cycle. International Journal of Hydrogen Energy. 2017;42(7):4673-8.
[41] Möller BF, Arriagada J, Assadi M, Potts I. Optimisation of an SOFC/GT system with CO2-capture. Journal of Power Sources. 2004;131(1-2):320-6.
[42] Calise F, d'Accadia MD, Vanoli L, Von Spakovsky M. Single-level optimization of a hybrid SOFC–GT power plant. Journal of Power Sources. 2006;159(2):1169-85.
[43] Behzadi A, Habibollahzade A, Zare V, Ashjaee M. Multi-objective optimization of a hybrid biomass-based SOFC/GT/double effect absorption chiller/RO desalination system with CO2 recycle. Energy conversion and management. 2019;181:302-18.

Table 1. Literature review of different optimization methods for SOFC/GT hybrid systems

Decision variables	Objective	Optimization Method	Application	Key Findings	Reference
SOFC fuel flow, operating temperature and pressure	Overall efficiency and power, total annual cost of power production and annual CO_2 emission	Pareto optimal employing EA optimizer	SOFC-GT	A set of optimal solution is presented	[9]
Fuel utilization, operating pressure of fuel cell, fuel and air flow	Capital cost, cost of electricity, CO_2 emissions, Power efficiency	MINSOOP algorithm employing NLP optimizer	Integrated Hybrid System	Overall efficiency achieved between 60-65%, CO_2 emissions between 0.30 - 0.32 kg/kWh	[22]
Air and fuel flows, cell voltage, air temperature	Power efficiency	Genetic Algorithm optimizer	SOFC-GT	Electrical efficiency is calculated above 60%.	[41]
Geometry and Operating Conditions	Overall plant cost	Genetic Algorithm using MATLAB	SOFC-GT	The most important variables to gain high efficiency and low costs are the pre-reforming ratio, heat exchanger area and SOFC active area	[42]
Temperature, Temp ratio and heat loss	Output power and efficiency	Thermodynamic analysis	SOFC-GT	Different parameters are analyzed to attain the maximum power and efficiency	[7]
Current density, pressure and temperature	Output power, efficiency of power and cost	Genetic Algorithm using MATLAB	SOFC-GT	Maximum power output of 108.33 kW and maximum efficiency of 63.93% are obtained at 0.51 $/kWh and 0.42$/kWh energy cost, respectively	[2]
Current density, FU, AU factor and pressure ratio	Exergy efficiency and SUCP	Genetic Algorithm using MATLAB	SOFC-GT	Optimal exergy efficiency is found 55.11%. Power production cost is calculated 24.68 $/GJ	[3]
Mass flow rate, temperature, number of cells, FU	Period of return and exergy efficiency	GA using MATLAB	SOFC-GT	Period of Return for SOFC-GT system is 9.88%, and the exergy efficiency is 40.93%	[4]

Compressor pressure ratio, combustion chamber inlet temperature, TIT, air current density, U_f, S/C ratio	Total cost rate and Exergy efficiency	NSGA-II algorithm using Interactive fuzzy multi-objective method	SOFC/GT Power plant	Minimum cost value is 0.0435 (USD/S) and exergy efficiency is 57.7 %	[30]
Current density, U_f, Stack temperature, pressure ratio, CO_2 recycle ratio	Exergy efficiency and total product cost	MOO-GA using MATLAB	Biomass fueled-SOFC/GT/RO desalination	exergy efficiency is 38.16% and product cost per unit is 69.47 $/GJ	[43]

Table 2. The model inlet parameters for the simulation of SOFC/GT system.

Parameter	Unit	Value
$\mathbf{T_{Stack}}$	℃	1000
P	bar	1
$\mathbf{U_{fuel}}$	%	85
$\mathbf{U_{air}}$	%	0.25
S/C ratio	-	2.5
$\mathbf{j}$	Am^{-2}	3200
$\mathbf{N_{Cell}}$	-	1152
$\mathbf{A_{Cell}}$	m^2	0.0834
$\mathbf{P_r}$	-	2.9

Table 3. Comparison of some simulation results of SOFC/GT system model with literature.

Parameter	Siemens-Westinghouse	Simulation results	Relative error (%)
Cell voltage (V)	0.610	0.607	-0.49
SOFC DC electrical power (kW)	187	187.53	0.28
SOFC AC electrical power (kW)	176	175.2	-0.45
GT-electrical power (kW)	47	43.04	-8.42
Net electrical power output (kW)	220	213.8	-2.81
Fist law Efficiency (%)	57	58.47	2.57

Table 4. The limitation of decision variables in MOO problem.

Parameter	Minimum	Maximum	Justification
Fuel utilization (%)	0.2	0.9	SOFC commercial range
Pressure ratio (bar)	2	5	Commercial restrictions
Steam to carbon ratio (S/C) (mol)	1	4	Methane reforming to hydrogen
Fuel flow rate (kg/s)	0.3	0.8	Economy of hybrid system

Table 5. The algorithm parameters.

PSO coefficient	Value	GA coefficient	Value
C_1, C_2	2	**Population**	30
W_{max}	30	**Mutiation**	0.01
W_{min}	1	**Crossover**	0.8

Table 6. The results of optimized key parameters of the system derived from PSO and GA algorithms.

Optimization Algorithm	**PSO**		**GA**	
Objective	**Energy efficiency**	**Output power**	**Energy efficiency**	**Output power**
Maximum value	88.2 %	419.2 kW	88 %	410.5 kW
Convergence iteration	47	39	51	56
Convergence time	507.2 s	432.8s	586.15 s	620.4 s
Fuel utilization	0.9	0.79	0.9	0.85
Pressure ratio	4.12	4.16	4.16	4.23
Steam to carbon ratio (S/C)	4	4	4	3.99
Fuel mass flow rate	0.3	0.9	0.3	0.8